Line Shapes in Coherent Ion Dip Spectroscopy of Polyatomic Molecules

R. Neuhauser,* R. Sussmann, and H. J. Neusser

Institut für Physikalische und Theoretische Chemie, Technische Universität München, Lichtenbergstrasse 4, D-85748 Garching, Germany

(Received 11 July 1994)

Using two narrow-band Fourier-transform limited, tunable ns laser pulses the observation of coherent adiabatic Raman processes becomes feasible for polyatomic molecules. Recent experiments reveal the possibility of an effective suppression of ionization in an ion dip experiment using a lambda-type resonant coherent optical-optical UV-double-resonance process and suggest its application in molecular spectroscopy. The experiments, including the observed ionization enhancement for off-resonance conditions, are quantitatively described using a few-level density matrix approach.

PACS numbers: 33.70.Jg, 33.80.Rv, 42.65.Dr

Coherent interaction of light with atoms leads to a variety of interesting phenomena such as dark resonances, trapping of population in a coherent superposition of quantum states, or effective population transfer experiments in multilevel systems [1–3]. After Fourier-transform limited ns UV-laser pulses have become available an extension of coherent techniques to molecular systems with additional internal degrees of freedom and a resulting higher level density with reactive channels is within the realm of possibilities.

One of the most interesting effects resulting from coherent atomic or molecular excitation with Fourier-transform limited laser pulses is the typical population dynamics encountered in a lambda-type three-level system (see Fig. 1) resonantly interacting with two laser pulses. Using a pump laser pulse for coherent coupling of levels 1 and 2 and a dump laser pulse coupling levels 2 and 3 with a typical time sequence and a coupling strength controlled by the Rabi frequencies $\Omega_{p,d}$ useful coherent population dynamics is expected: Recently, an adiabatic population transfer of nearly 100% from an initial level 1 to a final level 3 in the small molecule NO was experimentally achieved using a pulse sequence with a leading dump laser pulse followed by the slightly overlapping pump laser pulse [4]. In another experiment we showed that for fully resonant laser frequencies a nearly 100% suppression of resonant multiphoton ionization (REMPI) of the polyatomic molecule benzene is observed using the pulse sequence displayed in the lower part of Fig. 1 with a completely overlapping dump laser pulse [5]. Scanning the dump laser frequency while keeping the pump laser frequency in resonance is proposed to lead to a very sensitive rotationally resolving technique for high resolution spectroscopy of vibrationally excited states in the electronic ground state of polyatomic molecules and clusters. In this Letter we present density matrix calculations based on a simple model of the system that explain the experimental line shapes and show that, in agreement with new experimental results, not only ionization suppression but also an ionization enhancement can be expected.

The principle of the experimental setup is described in detail elsewhere [5]. Briefly, the linear polarized pump and dump laser pulses (see Fig. 1) are produced by the frequency-doubled output of two pulsed amplified single mode cw-laser beams with a FWHM linewidth of 60 MHz (dump laser) and 90 MHz (pump laser) in the UV spectral range. In our experiment the pump laser pulse with a duration of 10 ns completely overlaps in time with the stronger dump lase pulse of 20 ns duration.

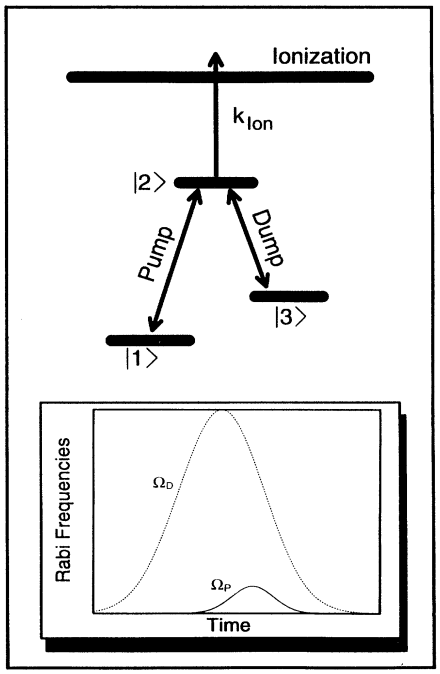

FIG. 1. Top: Level scheme of the investigated transitions in benzene. The pump laser pulse couples levels 1 and 2 with a Rabi frequency Ω_p while level 3 is coupled to level 2 by the dump laser pulse (Ω_d). Coupling of level 2 to the ionization continuum is included by a time-dependent decay rate k_{ion} due to incoherent ionization. Bottom: Rabi frequencies of the pump and the dump lasers as a function of time showing the special pulse sequence of the coherent ion dip experiment.

0031-9007/95/74(16)/3141(4)$06.00

This is different from recent stimulated Raman rapid adiabatic passage (STIRAP) experiments [4], although the important leading edge of the dump pulse is common for both cases. Both laser beams are focused into a cooled and collimated molecular beam with 1% benzene seeded in Ar. The ionized benzene molecules are mass separated from the additionally produced benzene-Ar cluster cations in a home-built time-of-flight mass spectrometer and detected with multichannel plates. This mass selective ionization detection is not necessary for high resolution spectroscopy of atoms and small molecules but is essential for high resolution spectroscopy of polyatomic molecules and molecular clusters as it yields a clear identification of the investigated species.

Figures 2 and 3 display the measured ion current signal at mass 78 u of benzene with fixed pump laser frequency ν_P but scanning the dump laser frequency ν_D across the transition $2 \rightarrow 3$, i.e., the $6_1, (J_K = 2_2) \leftarrow 1_2/5_2, (J_K = 3_3)^\dagger$, $\Delta K = +1$ transition of benzene. (Here J is the quantum number of total rotational angular momentum and K is its projection on the figure axis of the molecule. The symbol † denotes the transition to the higher lying state of the rotational level split by Darling-Dennisson coupling between the 5_2 and 1_2 vibrational states of the electronic ground state of benzene [6].)

In Fig. 2 the pump laser frequency is in resonance with the $2 \leftarrow 1$ transition. The nearly 90% dip in the ion current indicates the resonance of ν_D with the $2 \rightarrow 3$ transition when scanning the dump laser frequency (see inset of Fig. 2). This result is similar to our previous observations [5].

In a second experiment the pump laser frequency ν_P is detuned from resonance resulting in a lower ion current. Therefore, the spectrum of Fig. 3 was measured with increased detection sensitivity. If the dump laser frequency ν_D is now scanned across the $2 \rightarrow 3$ transition,

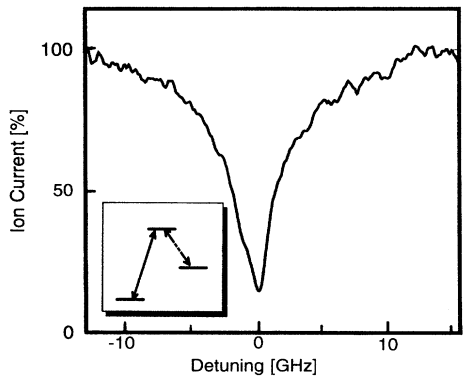

FIG. 2. Experimental ion current spectrum obtained when scanning the dump laser frequency ν_D. The frequency is given relative to the resonant frequency of the dump transition $2 \rightarrow 3$ that is found at 36 553.06(4) cm^{-1}. The 100% label on the y axis marks the maximum of the ion current for a completely off-resonant dump laser frequency.

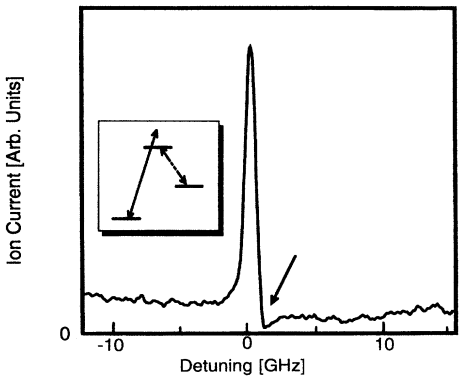

FIG. 3. Experimental ion current spectrum obtained when scanning the dump laser frequency ν_D. The frequency of the pump laser ν_P is fixed and detuned from the $2 \leftarrow 1$ transition as shown in the inset. Note the positive peak and the small dip marked by an arrow. The absolute height of the peak cannot be compared quantitatively to the off-resonant ion current of Fig. 2 due to the different detection sensitivity of the experimental setup used in both experiments.

two main features appear. First, there clearly exists a prominent positive peak in the ion current signal if the dump laser frequency is close to but not in exact resonance with the $2 \rightarrow 3$ transition. Second, a small dip marked by an arrow occurs in the even lower off-resonant ionization current signal.

Now we compare the experimental results of Fig. 3 with numerical calculations. These include the time development of the molecular density matrix considering the incoherent ionizing photon absorption step as an incoherent decay of level 2 [7]. Because of the high spectral resolution in our experiments, which results in selection of single rovibrational levels even in a large molecule, benzene, with a dense manifold of states, an effective lambda-type three-level system (see Fig. 1) can be used as a suitable base for theoretical modeling. This reduction to a few-level system using narrow-band laser systems is important for coherent ion dip spectroscopy: If some adjacent transitions from different initial ground state levels (e.g., with different J_K) to intermediate levels are not resolved, the resonance condition for the dump laser frequency may not be necessarily attainable simultaneously for all levels coupled by the light field. However, for the low rotational temperature of 1.3 K obtained in the molecular beam a sufficient spacing of the remaining rovibronic transitions can be expected for a wide class of polyatomic molecules.

The ionization rate k^i_{ion} out of level 2 (see Fig. 1) is proportional to the sum of squares of the time- and space-dependent Rabi frequencies $\Omega^i_p(r,t), \Omega^i_d(r,t)$ of the pump and the dump laser, respectively, as expected for an incoherent one-photon ionization process starting from level 2. As the ionization rate depends quadratically on the Rabi frequencies, ionization takes place mainly by

absorption of a photon from the more intense dump laser beam. Taking into account ionization after absorption of a photon from the weaker pump laser field yields no significant change of the line shape in our experiment and thus can be neglected. Using a phenomenological constant α the rate k^i_{ion} can be written as

$$k^i_{\text{ion}}(t,r) = \alpha \Omega^{i2}_d(t,r). \quad (1)$$

The time and the radial dependence of both Rabi frequencies is assumed to be Gaussian. The dependence on the symmetric top quantum numbers of the initial (J,K,m) and final states (J',K',m') of the transitions can be included in an effective Rabi frequency Ω^{eff} which is different for the various degenerate m subspaces [8]. (The quantum number m denotes the projection of the total rotational momentum J on a space-fixed axis.) With t denoting the time and r the radial distance from the laser beam axis the Rabi frequencies can be written as

$$\Omega^i_{p,d}(t,r) = \Omega^{\text{eff}}_{p,d}(J,J',K,K',m,m') \times \exp\left(-\frac{(t-\Delta t)^2}{\tau^2_{p,d}} - \frac{r^2}{\lambda^2_{p,d}}\right). \quad (2)$$

In Eq. (2) Δt is the small temporal delay of the laser pulses chosen in our experiment. No variation of the Rabi frequencies along the laser beam propagation axis is considered in this calculation since the diameter of the molecular beam is smaller than the Rayleigh range of the laser beam.

Since in our experiment with parallel and linearly polarized laser fields the $2J+1$ degenerate m subspaces are not coupled ($\Delta m = 0$), the population dynamics can be computed separately taking into account the m dependence of the effective Rabi frequency [8]. In this case a total ion signal Q is obtained by summing over the integrated ion currents resulting from the $2J+1$ different m subspaces:

$$Q = \sum_{i=-J}^{J} Q^i \sim \sum_{i=-J}^{J} \int dr \int dt\, k^i_{\text{ion}}(r,t)\rho^i_{22}(t,r). \quad (3)$$

Here $\rho^i_{22}(r,t)$ is the time- and space-dependent density matrix diagonal element of level 2 of the ith m subspace. It is obtained solving the time-dependent Liouville equation in the rotating wave approximation for different detuning of the laser frequencies and considering the time-dependent decay rate due to ionization out of level 2 [7]:

$$\frac{d}{dt}\hat{\rho} = i\frac{2\pi}{h}[\hat{H},\hat{\rho}] - \hat{\Gamma}(r,t). \quad (4)$$

Because of the inherent time dependence of pulsed excitation and ionization we decided to solve the equation numerically although analytic approaches are helpful for an intuitive understanding of the effects: An adiabatic-following approach in the framework of the dressed state picture can be applied as performed recently in coherent population transfer experiments [3]. Also an interpretation as an ac Stark shift caused by the *frequency-scanned,* stronger dump laser pulse and probed by the weaker pump laser at a *fixed* frequency is able to explain some features of the spectra. In the latter model the strong dump laser pulse causes a shift of level 2 depending on the detuning of ν_D from the $2 \rightarrow 3$ transition and the actual Rabi frequency Ω_D. Therefore, dependent on the detuning of the laser frequencies, the transition $2 \leftarrow 1$ can be shifted into resonance with the fixed pump laser frequency ν_P for some time during the strong dump laser pulse. However, the line shape of the expected peak depends in a complex way on time evolution and spatial variation of the Rabi frequencies. Using a numerical approach with $\Omega^{\text{eff}}_p(J,J',K,K',m'=m) = a_m(1.6\text{ GHz})$, $\Omega^{\text{eff}}_d(J,J',K,K',m'=m) = a_m(12.0\text{ GHz})$ with the m-dependent constant a_m ($a_0 = 0.293$, $a_{\pm 1} = 0.276$, $a_{\pm 2} = 0.218$), $\alpha = 1.8 \times 10^{-10}$ s, $t = 3.2 \times 10^{-9}$ s, $\lambda_p = \lambda_d = 140\ \mu$m, $\tau_p = 6.0 \times 10^{-9}$ s, $\tau_d = 12 \times 10^{-9}$ s as empirical parameters consistent with our knowledge of transition strength and laser intensities, we arrive at the calculated spectra shown in Fig. 4 for two different, fixed pump laser frequencies and varying dump laser frequencies. The value for α was found in reasonable agreement with known ionization rates of benzene

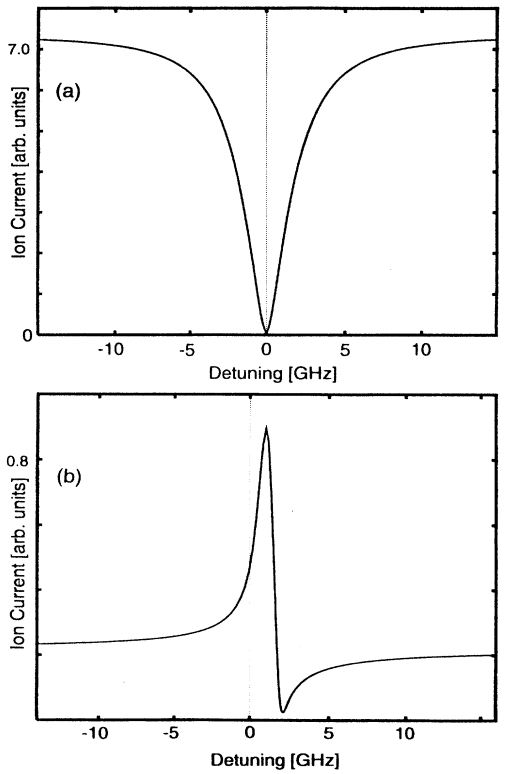

FIG. 4. Calculated spectra from a density matrix approach. (a) Pump laser frequency ν_P in resonance with the $2 \leftarrow 1$ transition and dump laser frequency ν_D scanned. (b) Pump laser frequency ν_P detuned by 2000 MHz from the $2 \leftarrow 1$ transition and dump laser frequency ν_D scanned.

determined from incoherent two-photon ionization experiments [9].

In Fig. 4(a) the theoretical result is shown if the pump laser frequency ν_P is in resonance with the $2 \leftarrow 1$ transition and the dump laser frequency ν_D is scanned. The large depth of the ion dip as well as the line shape are typical results and in line with the experimental results shown in Fig. 2. The line shape results from the integration over the spatial distribution of Rabi frequencies Ω_P, Ω_D and a summation over the different molecule orientations ($m = 0, \pm 1, \pm 2$).

In Fig. 4(b) the theoretical spectrum is shown obtained by solving the Liouville equation for a slightly detuned pump laser frequency ν_P (detuning $\Delta_p = 2000$ MHz to the blue of the $2 \leftarrow 1$ transition) and a scanned dump laser frequency ν_D. Here the small dip as well as the increase in ion signal, both striking features of the experimental spectrum of Fig. 3, are well reproduced. A small background pedestal of the ion current is present since the detuning Δ_p is still comparable to the maximum Rabi frequencies in the central area of the laser beams. An intuitive interpretation of the peak and its principal shape is possible in the ac Stark shift model mentioned before. An exact analytic discussion of the line shape (linewidth, peak height, etc.) containing the spatially and temporally varying Rabi frequencies is difficult because of the complex response of the system. The asymmetric small dip to the right of the peak indicates the occurrence of the Raman resonance $1 \rightarrow 3$.

Numerical evolutions show that the width of the dip in Fig. 4(a) as well as the relative height and width of the peak in Fig. 4(b) depend critically on the chosen ionization parameter α and the absolute values of the Rabi frequencies Ω_d^i, Ω_p^i. However, the principal line shape is not changed significantly if Rabi frequencies are changed but their ratio Ω_P/Ω_D is kept constant.

In conclusion, we have investigated the $0_0 \rightarrow 5_2/1_2^+$ transition in the polyatomic molecule benzene using the new mass selective double resonance technique of coherent ion dip spectroscopy. We found not only ionization suppression but also ionization enhancement depending on the degree of detuning of the pump laser frequency from the $2 \leftarrow 1$ transition. Solving numerically the density matrix equations, which describe the coherent response of the system, a simulation of the experimental spectra was possible. This understanding of the different line shapes and the sharp peak positions based on a simple model will be helpful for future applications of the coherent ion dip spectroscopy to polyatomic molecules and clusters including strong coupling of excited light levels to dark background states.

Financial support from the Deutsche Forschungsgemeinschaft is gratefully acknowledged.

*Electronic address: robert@pluto.phys.chemie.tu-muenchen.de

[1] G. Alzetta, A. Gozzini, L. Moi, and G. Orriols, Nuovo Cimento Soc. Ital. Fis. **36B**, 5 (1976); E. Arimondo and G. Orriols, Lett. Nuovo Cimento **17**, 333 (1976); N. R. Gray, R. M. Whitley, and C. R. Stroud, Jr., Opt. Lett. **3**, 218 (1976); K. J. Boller, A. Imamoglu, and S. E. Harris, Phys. Rev. Lett. **66**, 2593 (1991).

[2] D. Grischkowsky and M. M. T. Loy, Phys. Rev. A **12**, 1117 (1975); C. Liedenbaum, S. Stolte, and J. Reuss, Phys. Rep. **178**, 1 (1989); N. Dam, S. Stolte, and J. Reuss, Chem. Phys. **135**, 437 (1989); U. Gaubatz, P. Rudecki, S. Schiemann, and K. Bergmann, J. Chem. Phys. **92**, 5363 (1990); N. Dam, S. Stolte, and J. Reuss, Chem Phys. **140**, 217 (1990).

[3] J. Oreg, F. T. Hioe, and J. H. Eberly, Phys. Rev. A **29**, 690 (1984); Y. B. Band, Phys. Rev. A **45**, 6643 (1992); B. Gloshko and B. Kryzhanovsky, Phys. Rev. A **46**, 2823 (1992).

[4] S. Schiemann, A. Kuhn, S. Steuerwald, and K. Bergmann, Phys. Rev. Lett. **71**, 3637 (1993).

[5] R. Sussmann, R. Neuhauser, and H. J. Neusser, J. Chem. Phys. **100**, 4784 (1994).

[6] B. T. Darling and D. M. Dennison, Phys. Rev. **57**, 128 (1940); Th. Weber, E. Riedle, and H. J. Neusser, J. Opt. Soc. Am. B **7**, 1877 (1990).

[7] A. T. Georges and P. Lambropoulos, Phys. Rev. A **18**, 587 (1978); L. B. Bigio, G. S. Ezra, and E. R. Grant, J. Chem. Phys. **83**, 5369 (1985); G. W. Coulston and K. Bergmann, J. Chem. Phys. **96**, 3467 (1992).

[8] Y. H. Band and P. S. Julienne, J. Chem. Phys. **96**, 3339 (1992); L. C. Biedenharn and J. D. Louck, *Angular Momentum in Quantum Physics* (Addison-Wesley, Reading, MA, 1981); N. Dam, L. Oudejans, and J. Reuss, Chem. Phys. **140**, 217 (1990).

[9] U. Boesl, H. J. Neusser, and E. W. Schlag, Chem. Phys. **55**, 193 (1981).